

February 1996
 DOE/ER/40762-080
 U.MD. PP#96-067
 ADP-96-9/T214

Neutron Structure Functions From Nuclear Data *

W.Melnitchouk

Department of Physics, University of Maryland, College Park, MD 20742

A.W.Thomas

Department of Physics and Mathematical Physics, University of Adelaide, 5005, Australia.

Abstract

The spin-averaged structure function of the neutron, F_2^n , is extracted from recent deuteron data, taking into account the small but significant corrections from nuclear effects in the deuteron. At small x , the F_2^D/F_2^p ratio measured by the New Muon and Fermilab E665 Collaborations is interpreted to suggest a small amount of shadowing in deuterium, which acts to enhance F_2^n for $x \lesssim 0.1$. A careful treatment of Fermi motion, binding and nucleon off-shell effects in the deuteron also indicates that the neutron/proton structure function ratio as $x \rightarrow 1$ is consistent with the perturbative QCD expectation of $3/7$, but larger than the traditional value of $1/4$.

I. INTRODUCTION

The quark structure of the nucleon is one of the most fundamental aspects of hadron physics. Deep inelastic scattering (DIS) of leptons from hydrogen has yielded a wealth of information on the quark and gluon substructure of the proton. The absence of free neutron targets means, however, that it is difficult to obtain direct data on F_2^n . As a result, one usually uses deuterium targets, and extracts neutron structure information from a knowledge of the proton structure function, and the nucleon wave function in the deuteron. The accuracy of the extracted neutron data naturally depends on the level of understanding of the nuclear physics in the deuteron, as well as on the extraction procedure itself. Both of these issues are carefully addressed in this paper.

*Invited talk presented by W. Melnitchouk at the *Cracow Epiphany Conference on Proton Structure*, 5-6 Jan. 1996, Cracow, Poland. To appear in *Acta Phys. Pol.*

The treatment of nuclear effects is divided into two regions: large x ($x \gtrsim 0.3$) and small x ($x \lesssim 0.2$). In the context of the multiple scattering framework, the large- x effects are described within the impulse approximation, in which the virtual photon interacts with only one nucleon in the deuteron, while the other nucleon remains spectator to the interaction. The impulse approximation provides a natural framework within which effects from nuclear binding, Fermi motion, and nucleon off-shellness can be incorporated. At small x , on the other hand, there are important contributions from the rescattering of the probe from both nucleons in the deuteron, which gives rise to the phenomenon known as nuclear shadowing.

II. LARGE X

Away from the small- x region ($x \gtrsim 0.3$), the dominant contribution to the deuteron structure function can be computed from the impulse approximation. Here the total γ^*D amplitude is factorized into γ^*N and ND amplitudes, although, contrary to what is often assumed, this factorization does not automatically lead to a factorization of cross sections in the convolution model [1].

A. Binding, Fermi Motion and Off-Shell Effects

Starting from the impulse approximation, one can show that in the non-relativistic approximation the nuclear structure function can be written in convolution form, in which the structure function of the nucleon is smeared with a momentum distribution, $f_{N/D}(y)$, of nucleons in the deuteron [1,2]:

$$F_2^{D \text{ (conv)}}(x, Q^2) = \int dy f_{N/D}(y) F_2^N\left(\frac{x}{y}, Q^2\right), \quad (1)$$

where $F_2^N = F_2^p + F_2^n$. Equation (1) is correct to order $(v/c)^2$ (with v the nucleon velocity), provided we also neglect the possible p^2 dependence in the nucleon structure function. The distribution function $f_{N/D}(y)$ is determined by the deuteron wave functions u, w, v_t and v_s [3] (corresponding to the deuteron's S, D and triplet and singlet P waves) [4]:

$$f_{N/D}(y) = \frac{M_D}{4} y \int_{-\infty}^{p_{max}^2} dp^2 \frac{E_p}{p_0} \left(u^2(\mathbf{p}^2) + w^2(\mathbf{p}^2) + v_t^2(\mathbf{p}^2) + v_s^2(\mathbf{p}^2) \right) \quad (2)$$

where p is the interacting nucleon's four-momentum, with a maximum squared value $p_{max}^2 = yM_D^2 - yM^2/(1-y)$, and $E_p = \sqrt{M^2 + \mathbf{p}^2}$.

As explained in Refs. [4,5], explicit corrections to Eq.(1), which cannot be written in convolution form, arise when the bound nucleons' off-mass-shell structure is taken into account:

$$F_2^D(x, Q^2) = F_2^{D \text{ (conv)}}(x, Q^2) + \delta^{(\text{off})} F_2^D(x, Q^2). \quad (3)$$

The correction $\delta^{(\text{off})} F_2^D$ receives contributions from the off-shell components in the deuteron wave function, as well as from the off-mass-shell dependence of the bound nucleon structure function [4] (i.e. in the $p^2 \rightarrow M^2$ limit, in which the P -state wave functions also vanish, one has $\delta^{(\text{off})} F_2^D \rightarrow 0$).

FIGURES

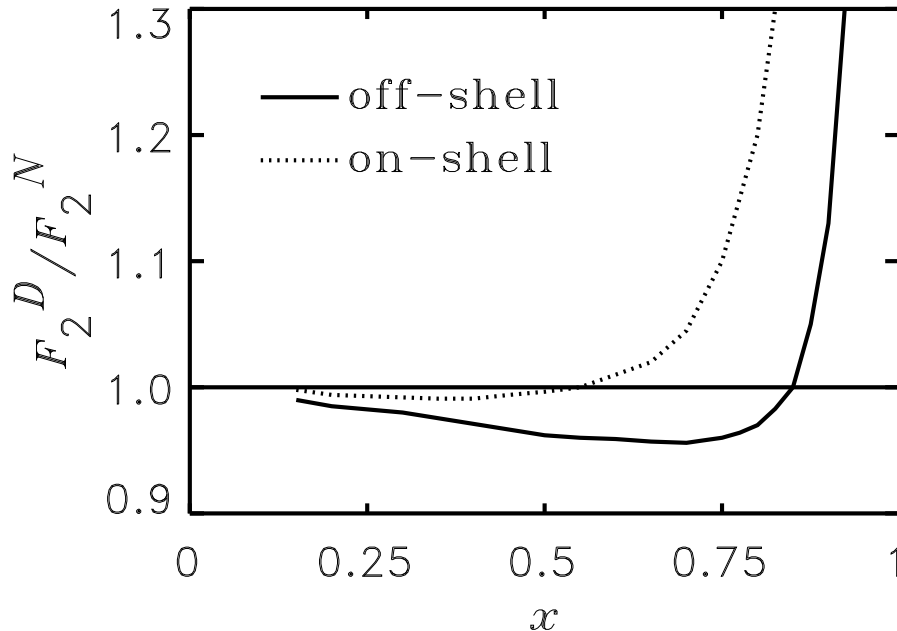


FIG. 1. F_2^D/F_2^N ratio as a function of x for the off-shell model of Refs. [4,5] (solid) and the on-shell model of Ref. [6] (dotted).

In Refs. [4,5] the structure function F_2^N was modeled in terms of relativistic quark–nucleon vertex functions, which were parametrized by comparing with available data for the parton distribution functions. The off-shell extrapolation of the γ^*N interaction was modeled assuming no additional dynamical p^2 dependence in the quark–nucleon vertices. This enabled an estimate of the correction $\delta^{(\text{off})}F_2^D$ to be made, which was found to be quite small, of the order $\sim 1-2\%$ for $x \lesssim 0.9$. The result of the fully off-shell calculation from Ref. [4] is shown in Fig.1 (solid curve), where the ratio of the total deuteron to nucleon structure functions (F_2^D/F_2^N) is plotted. Shown also is the result of an on-mass-shell calculation from Ref. [6] (dotted curve), which has been used in many previous analyses of the deuteron data [7,8]. The most striking difference between the curves is the fact that the on-shell ratio has a very much smaller trough at $x \approx 0.3$, and rises faster above unity (at $x \approx 0.5$) than the off-shell curve, which has a deeper trough, at $x \approx 0.6-0.7$, and rises above unity somewhat later (at $x \approx 0.8$).

The behavior of the off-shell curve in Fig.1 is qualitatively similar to that found by Uchiyama and Saito [9], Kaptari and Umnikov [10], and Braun and Tokarev [11], who also used off-mass-shell kinematics, but did not include the (small) non-convolution correction term $\delta^{(\text{off})}F_2^D$. The on-shell calculation [6], on the other hand, was performed in the infinite momentum frame where the nucleons are on their mass shells and the physical structure functions can be used in Eq.(1). One problem with this approach is that the deuteron wave functions in the infinite momentum frame are not explicitly known. In practice one usually makes use of the ordinary non-relativistic S - and D -state deuteron wave functions

calculated in the deuteron rest frame, a procedure which is analogous to including only Fermi motion effects in the deuteron. In addition, one knows that the effect of binding in the infinite momentum frame shows up in the presence of additional Fock components (e.g. NN -meson(s)) in the nuclear wave function, which have not yet been computed.

Clearly, a smaller D/N ratio at large x , as in the off-shell calculation, implies a larger neutron structure function in this region. To estimate the size of the effect on the n/p ratio requires one to “deconvolute” Eq.(1) in order to extract F_2^n .

B. Extraction of F_2^n

To study nuclear effects on the neutron structure function arising from different models of the deuteron, one must eliminate any effects that may arise from the extraction method itself. We therefore use exactly the same extraction procedure as used in previous SLAC [7] and EMC [8] data analyses, namely the smearing (or deconvolution) method discussed by Bodek *et al.* [12]. This method involves the direct use of the proton and deuteron *data*, without making any assumption for F_2^n itself. For completeness let us briefly outline the main ingredients in this method. (For alternative methods of unfolding the neutron structure function see for example Refs. [13,14].)

Firstly, one subtracts from the deuteron data, F_2^D , the additive, off-shell corrections, $\delta^{(\text{off})} F_2^D$, to give the convolution part, $F_2^{D(\text{conv})}$. Then one smears the proton data, F_2^p , with the nucleon momentum distribution function $f_{N/D}(y)$ in Eq.(1) to give $\tilde{F}_2^p \equiv F_2^p/S_p$. The smeared neutron structure function, \tilde{F}_2^n , is then obtained from

$$\tilde{F}_2^n = F_2^{D(\text{conv})} - \tilde{F}_2^p. \quad (4)$$

Since the smeared neutron structure function is defined as $\tilde{F}_2^n \equiv F_2^n/S_n$, we can invert this to obtain the structure function of a free neutron,

$$F_2^n = S_n \left(F_2^{D(\text{conv})} - F_2^p/S_p \right). \quad (5)$$

The proton smearing factor, S_p , can be computed at each x from the function $f_{N/D}(y)$, and a parametrization of the F_2^p data (for example, the recent fit in Ref. [15] to the combined SLAC, BCDMS and NMC data). The neutron F_2^n structure function is then derived from Eq.(5) taking as a first guess $S_n = S_p$. These values of F_2^n are then smeared by the function $f_{N/D}(y)$, and the results used to obtain a better estimate for S_n . The new value for S_n is then used in Eq.(5) to obtain an improved estimate for F_2^n , and the procedure repeated until convergence is achieved.

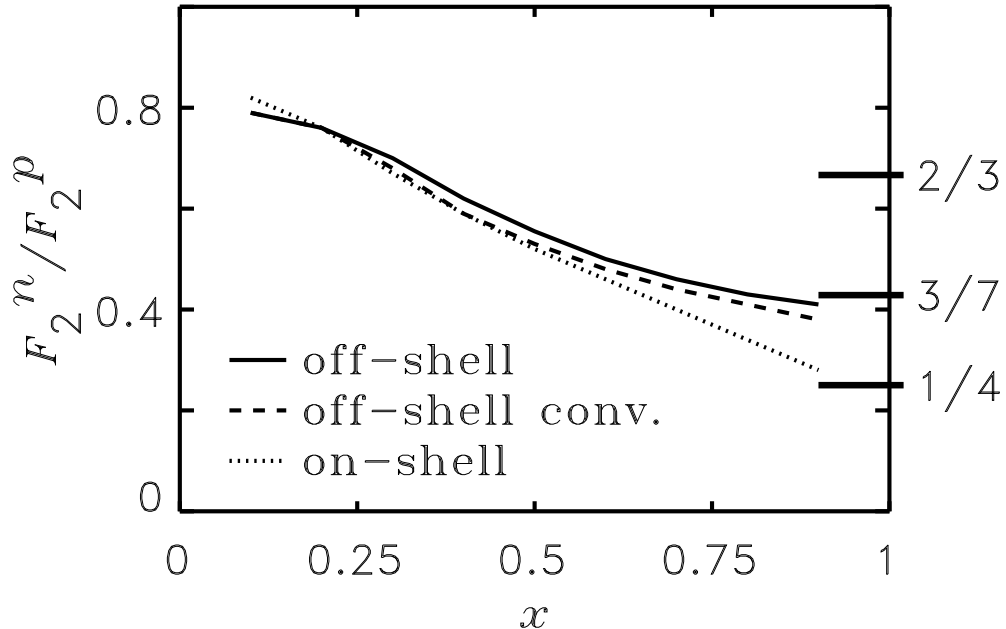


FIG. 2. F_2^n/F_2^p ratio as a function of x , for the off-shell model (solid), off-shell model without the convolution-breaking term (dashed), and the on-shell model (dotted). On the right-hand axis are marked the $x \rightarrow 1$ limits of the SU(6) symmetric model (2/3), and the predictions of the models of Refs. [17,18] (1/4) and [20,21] (3/7).

The results of this procedure for F_2^n/F_2^p are presented in Fig.2, for both the off-shell calculation (solid) and the on-shell model (dotted). The increase in the off-shell ratio at large x is a direct consequence of the deeper trough in the F_2^D/F_2^N ratio in Fig.1. To illustrate the role of the non-convolution correction, $\delta^{(\text{off})} F_2^D$, we have also performed the analysis setting this term to zero, and approximating F_2^D by $F_2^{D(\text{conv})}(x)$. The effect of this correction (dashed curve in Fig.2) appears minimal. One can therefore attribute most of the difference between the off- and on-shell results to kinematics, since both calculations involve very similar deuteron wave functions.

Before discussing the implications of these results, let us briefly outline the connection between structure functions at large x and the breaking of SU(6) spin-flavor symmetry.

C. SU(6) Symmetry Breaking

The large- x region, being valence quark dominated, is where SU(6) symmetry breaking effects in valence quark distributions should be most prominent. The precise mechanism for the breaking of the spin-flavor SU(6) symmetry is a basic question in hadronic physics. In a world of exact SU(6) symmetry, the wave function of a proton, polarized say in the $+z$ direction, would be simply [16]:

$$p \uparrow = \frac{1}{\sqrt{2}} u \uparrow (ud)_{S=0} + \frac{1}{\sqrt{18}} u \uparrow (ud)_{S=1} - \frac{1}{3} u \downarrow (ud)_{S=1}$$

$$-\frac{1}{3}d\uparrow(uu)_{S=1} - \frac{\sqrt{2}}{3}d\downarrow(uu)_{S=1}, \quad (6)$$

where the subscript S denotes the total spin of the two-quark component. In this limit, apart from charge and flavor quantum numbers, the u and d quarks in the proton would be identical. The nucleon and Δ isobar would, for example, be degenerate in mass. In deep-inelastic scattering, exact SU(6) symmetry would be manifested in equivalent shapes for the valence quark distributions of the proton, which would be related simply by $u_V(x) = 2d_V(x)$ for all x . For the neutron to proton structure function ratio this would imply:

$$\frac{F_2^n}{F_2^p} = \frac{2}{3} \quad [\text{SU(6) symmetry}]. \quad (7)$$

In nature spin-flavor SU(6) symmetry is, of course, broken. The nucleon and Δ masses are split by some 300 MeV. Furthermore, with respect to DIS, it is known that the d quark distribution is softer than the u quark distribution, with the neutron/proton ratio deviating at large x from the SU(6) expectation. The correlation between the mass splitting in the **56** baryons and the large- x behavior of F_2^n/F_2^p was observed some time ago by Close [17] and Carlitz [18]. Based on phenomenological [17] and Regge [18] arguments, the breaking of the symmetry in Eq.(6) was argued to arise from a suppression of the “diquark” configurations having $S = 1$ relative to the $S = 0$ configuration, namely

$$(qq)_{S=0} \gg (qq)_{S=1}, \quad x \rightarrow 1. \quad (8)$$

Such a suppression is in fact quite natural if one observes that whatever mechanism leads to the observed $N - \Delta$ splitting (e.g. color-magnetic force, instanton-induced interaction, pion exchange), it necessarily acts to produce a mass splitting between the two possible spin states of the two quarks, $(qq)_S$, which act as spectators to the hard collision, with the $S = 1$ state heavier than the $S = 0$ state by some 200 MeV [19]. From Eq.(6), a dominant scalar valence diquark component of the proton suggests that in the $x \rightarrow 1$ limit F_2^p is essentially given by a single quark distribution (i.e. the u), in which case:

$$\frac{F_2^n}{F_2^p} \rightarrow \frac{1}{4}, \quad \frac{d}{u} \rightarrow 0 \quad [S = 0 \text{ dominance}]. \quad (9)$$

This expectation has, in fact, been built into many phenomenological fits to the parton distribution data.

An alternative suggestion, based on perturbative QCD, was originally formulated by Farrar and Jackson [20]. There it was argued that the exchange of longitudinal gluons, which are the only type permitted when the spins of the two quarks in $(qq)_S$ are aligned, would introduce a factor $(1-x)^{1/2}$ into the Compton amplitude — in comparison with the exchange of a transverse gluon between quarks with spins anti-aligned. In this approach the relevant component of the proton valence wave function at large x is that associated with states in which the total “diquark” spin *projection*, S_z , is zero:

$$(qq)_{S_z=0} \gg (qq)_{S_z=1}, \quad x \rightarrow 1. \quad (10)$$

Consequently, scattering from a quark polarized in the opposite direction to the proton polarization is suppressed by a factor $(1-x)$ relative to the helicity-aligned configuration.

A similar result is also obtained in the treatment of Brodsky *et al.* [21] (based on counting-rules), where the large- x behavior of the parton distribution for a quark polarized parallel ($\Delta S_z = 1$) or antiparallel ($\Delta S_z = 0$) to the proton helicity is given by: $q^{\uparrow\downarrow}(x) = (1 - x)^{2n-1+\Delta S_z}$, where n is the minimum number of non-interacting quarks (equal to 2 for the valence quark distributions). In the $x \rightarrow 1$ limit one therefore predicts:

$$\frac{F_2^n}{F_2^p} \rightarrow \frac{3}{7}, \quad \frac{d}{u} \rightarrow \frac{1}{5} \quad [S_z = 0 \text{ dominance}]. \quad (11)$$

Note that the d/u ratio *does not vanish* in this model. Clearly, if one is to understand the dynamics of the nucleon's quark distributions at large x , it is imperative that the consequences of these models be tested experimentally.

The reanalyzed SLAC [7,22] data points themselves are plotted in Fig.3, at an average value of $Q^2 \approx 12 \text{ GeV}^2$. The very small error bars are testimony to the quality of the SLAC p and D data. The data represented by the open circles have been extracted with the on-shell deuteron model of Ref. [6], while the filled circles were obtained using the off-shell model of Refs. [4,5]. Most importantly, the F_2^n/F_2^p points obtained with the off-shell method appear to approach a value broadly consistent with the Farrar-Jackson [20] and Brodsky *et al.* [21] prediction of $3/7$, whereas the data previously analyzed in terms of the on-shell formalism produced a ratio that tended to the lower value of $1/4$.

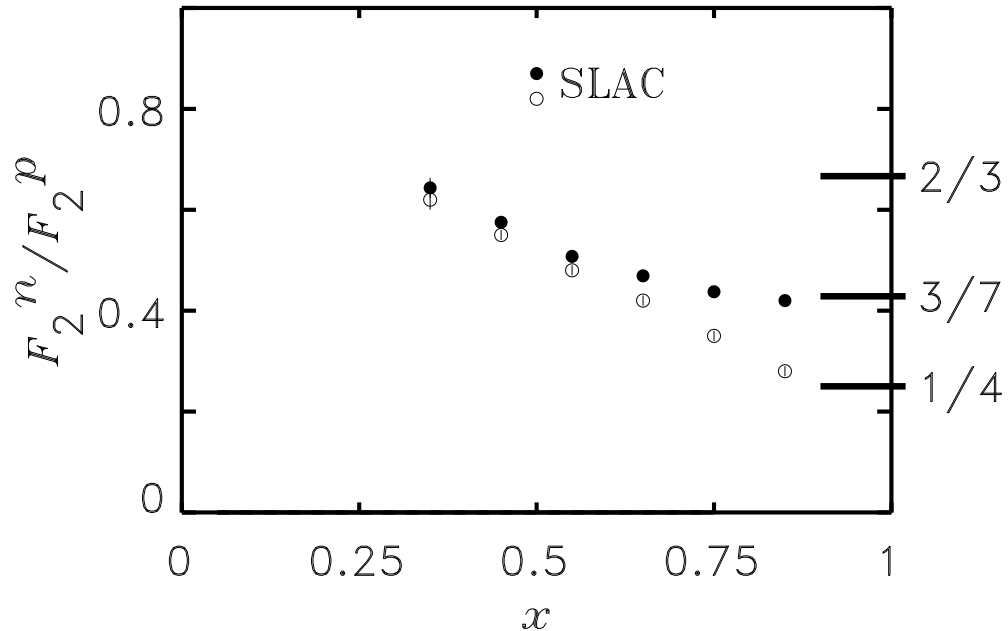


FIG. 3. Deconvoluted F_2^n/F_2^p ratio extracted from the SLAC p and D data [7,22], at an average value of $Q^2 \approx 12 \text{ GeV}^2$, assuming no off-shell effects (open circles), and including off-shell effects (full circles).

The d/u ratio, shown in Fig.4, is obtained by inverting F_2^n/F_2^p in the valence quark dominated region. The points extracted using the off-shell formalism (solid circles) are

again significantly above those obtained previously with the aid of the on-shell prescription. In particular, they indicate that the d/u ratio may actually approach a *finite* value in the $x \rightarrow 1$ limit, contrary to the expectation of the model of Refs. [17,18], in which d/u tends to zero. Although it is *a priori* not clear at which scale the model predictions [17,18,20,21] should be valid, for the values of Q^2 corresponding to the analyzed data the effects of Q^2 evolution are minimal.

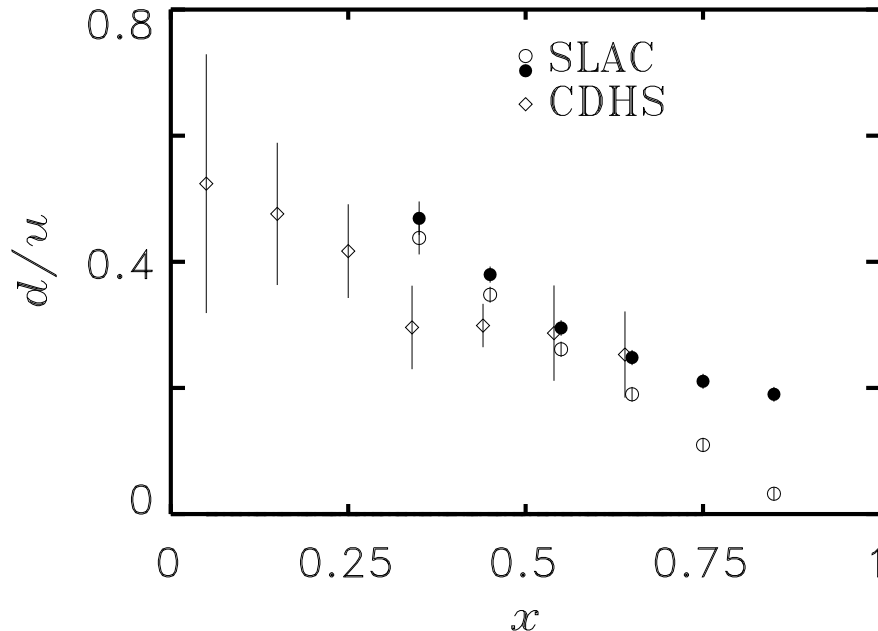


FIG. 4. Extracted d/u ratio, using the off-shell deuteron calculation (full circles) and using on-shell kinematics (open circles). Also shown for comparison is the ratio extracted from neutrino measurements by the CDHS collaboration [23].

Naturally it would be preferable to extract F_2^n at large x without having to deal with uncertainties in the nuclear effects. In principle this could be achieved by using neutrino and antineutrino beams to measure the u and d distributions in the proton separately, and reconstructing F_2^n from these. Unfortunately, as seen in Fig.4, the neutrino data from the CDHS collaboration [23] do not extend out to very large x ($x \lesssim 0.6$), and at present cannot discriminate between the different methods of analyzing the electron–deuteron data.

The results of our off-shell model are qualitatively similar [22] to those obtained using the nuclear density method suggested by Frankfurt and Strikman [24]. There the EMC effect in deuterium was assumed to scale with that in heavier nuclei according to the ratio of the respective nuclear densities, so that the ratio F_2^D/F_2^N in the trough region was depleted by about 4%, similar to that in Fig.1 (solid curve). This would give an F_2^n/F_2^p ratio broadly consistent with 3/7.

We should also point out similar consequences for the spin-dependent neutron structure function g_1^n , where the models of Refs. [17,18] and Refs. [20,21] also give different predictions for g_1^n/g_1^p as $x \rightarrow 1$, namely 1/4 and 3/7, respectively. Quite interestingly, while the ratio of

polarized to unpolarized u quark distribution is predicted to be the same in the two models,

$$\frac{\Delta u}{u} \rightarrow 1 \quad [S = 0 \text{ or } S_z = 0 \text{ dominance}], \quad (12)$$

the results for the d -quark distribution ratio differ even in sign:

$$\frac{\Delta d}{d} \rightarrow -\frac{1}{3} \quad [S = 0 \text{ dominance}], \quad (13a)$$

$$\rightarrow 1 \quad [S_z = 0 \text{ dominance}]. \quad (13b)$$

To extract information on the polarized parton densities at large x that is capable of discriminating between these predictions, the same care will need to be taken when subtracting the nuclear effects from g_1^D and g_1^{3He} . In particular, the results of Refs. [2,25] indicate that while the simple prescription [26] of subtracting the g_1^p structure function from the D data, modified only by the deuteron D -state probability, is surprisingly good for $x \lesssim 0.6$, it is completely inadequate for $x \gtrsim 0.7$.

Having seen that how one handles nuclear corrections can critically affect the deciphering of the physical implications of the extracted structure function at large x , we now examine the consequences of nuclear effects in deuterium in the small- x region.

III. SMALL x

At small values of x the impulse approximation should eventually break down. Indeed, one finds that coherent multiple scattering effects become very important when the characteristic time scale $1/Mx$ of the DIS process becomes larger than the typical average distance between bound nucleons in the nucleus, which occurs typically for $x \lesssim 0.1$. These effects are seen, for example, in the low- x depletion of the nuclear EMC ratio, F_2^A/F_2^D . Any shadowing in the deuteron itself should therefore produce a depletion in the F_2^D/F_2^N ratio at small x [27–32].

A. Nuclear Shadowing

The rescattering of the virtual photon from several nucleons in a nucleus is usually described within the non-relativistic Glauber multiple scattering formalism. Relativistic corrections will amount to a few percent out of a shadowing correction to F_2^D that will itself be a few percent in total, and hence can be neglected. For the deuteron the only contribution in the Glauber series comes from the double scattering process.

At small x , nuclear binding and Fermi motion corrections can be neglected, and the total deuteron structure function written as:

$$F_2^D(x, Q^2) \approx F_2^p(x, Q^2) + F_2^n(x, Q^2) + \delta^{(\text{shad})} F_2^D(x, Q^2). \quad (14)$$

In modeling the shadowing correction, $\delta^{(\text{shad})} F_2^D$, our approach is to take a two-phase model, similar to that of Kwiecinski and Badelek [27–29]. At high virtuality the interaction of the virtual photon with the nucleus is parametrized in terms of diffractive scattering through

the double and triple Pomeron, as well as scattering from exchanged mesons in the deuteron. On the other hand, at low virtuality it is most natural to apply a vector meson dominance (VMD) model, in which the virtual photon interacts with the nucleons via its hadronic structure, namely the ρ^0 , ω and ϕ mesons. The latter contribution vanishes at sufficiently high Q^2 , but for $Q^2 \lesssim 1 \text{ GeV}^2$ it is in fact responsible for the majority of the Q^2 variation.

For the diffractive component, Pomeron (IP) exchange between the projectile and two or more constituent nucleons models the interaction of partons from different nucleons within the deuteron. Assuming factorization of the diffractive cross section, the shadowing correction (per nucleon) to the deuteron structure function F_2^D from IP -exchange is written as a convolution of the Pomeron structure function, F_2^{IP} , with a distribution function (“flux factor”), $f_{IP/D}$, describing the number density of exchanged Pomerons:

$$\delta^{(IP)} F_2^D(x, Q^2) = \int_{y_{min}}^2 dy f_{IP/D}(y) F_2^{IP}(x_{IP}, Q^2), \quad (15)$$

where, within the non-relativistic approximation [27–31],

$$f_{IP/D}(y) = -\frac{\sigma_{pp}}{8\pi^2} \frac{1}{y} \int d^2\mathbf{k}_T S_D(\mathbf{k}^2). \quad (16)$$

Here $y = x(1 + M_X^2/Q^2)$ the light-cone momentum fraction carried by the Pomeron (M_X is the mass of the diffractive hadronic debris), and $x_{IP} = x/y$ is the momentum fraction of the Pomeron carried by the struck quark in the Pomeron. The deuteron form factor, $S_D(\mathbf{k}^2)$, is given in terms of the coordinate space wave functions:

$$S_D(\mathbf{k}^2) = \int_0^\infty dr \left(u^2(r) + w^2(r) \right) j_0(|\mathbf{k}|r), \quad (17)$$

where j_0 is the spherical Bessel function. Within experimental errors, the factorization hypothesis, as well as the y dependence of $f_{IP/A}(y)$ [27–31], are consistent with the recent HERA data [33] obtained from observations of large rapidity gap events in diffractive ep scattering. These data also confirm previous findings that the Pomeron structure function contains both a hard and a soft component: $F_2^{IP}(x_{IP}, Q^2) = F_2^{IP(\text{hard})}(x_{IP}, Q^2) + F_2^{IP(\text{soft})}(x_{IP}, Q^2)$. The hard component of F_2^{IP} is generated from an explicit $q\bar{q}$ component of the Pomeron, and has an x_{IP} dependence given by $x_{IP}(1 - x_{IP})$ [34], in agreement with the recent diffractive data [33]. The soft part, which is driven at small x_{IP} by the triple-Pomeron interaction [27], has a sea quark-like x_{IP} dependence, with normalization fixed by the triple-Pomeron coupling constant.

The dependence of F_2^{IP} on Q^2 at large Q^2 arises from radiative corrections to the parton distributions in the Pomeron [28], which leads to a weak, logarithmic, Q^2 dependence for the shadowing correction $\delta^{(IP)} F_2^D$. The low- Q^2 extrapolation of the $q\bar{q}$ component is parametrized by applying a factor $Q^2/(Q^2 + Q_0^2)$, where $Q_0^2 \approx 0.485 \text{ GeV}^2$ [35] may be interpreted as the inverse size of partons inside the virtual photon. For the nucleon sea quark densities relevant for $F_2^{IP(\text{soft})}$ we use the recent parametrization from Ref. [35], which includes a low- Q^2 limit consistent with the real photon data, in which case the total Pomeron contribution $\delta^{(IP)} F_2^D \rightarrow 0$ as $Q^2 \rightarrow 0$.

To adequately describe shadowing for small Q^2 requires one to use a higher-twist mechanism, such as vector meson dominance. VMD is empirically based on the observation that

some aspects of the interaction of photons with hadronic systems resemble purely hadronic interactions. In terms of QCD this is understood in terms of a coupling of the photon to a correlated $q\bar{q}$ pair of low invariant mass, which may be approximated as a virtual vector meson. One can then estimate the amount of shadowing in terms of the multiple scattering of the vector meson using Glauber theory. The corresponding correction (per nucleon) to the nuclear structure function is:

$$\delta^{(V)} F_2^D(x, Q^2) = \frac{Q^2}{\pi} \sum_V \frac{\delta\sigma_{VD}}{f_V^2(1 + Q^2/M_V^2)^2}, \quad (18)$$

where

$$\delta\sigma_{VD} = -\frac{\sigma_{VN}^2}{8\pi^2} \int d^2\mathbf{k}_T S_D(\mathbf{k}^2) \quad (19)$$

is the shadowing correction to the vector meson—nucleus cross section, f_V is the photon—vector meson coupling strength, and M_V is the vector meson mass.

In practice, only the lowest mass vector mesons ($V = \rho^0, \omega, \phi$) are important at low Q^2 . For $Q^2 \rightarrow 0$ and fixed x , $\delta^{(V)} F_2^D$ disappears due to the vanishing of the total F_2^D . Furthermore, since this is a higher twist effect, shadowing in the VMD model dies off quite rapidly between $Q^2 \sim 1$ and 10 GeV^2 , so that for $Q^2 \gtrsim 10 \text{ GeV}^2$ it is almost negligible — leaving only the diffractive term, $\delta^{(IP)} F_2^D$. (Note that at fixed ν , for decreasing Q^2 the ratio F_2^D/F_2^p approaches the photoproduction limit.)

Another potential source of shadowing arises from the exchange of mesons between the nucleons and the probe. It has previously been suggested [36] that this leads to some *antishadowing* corrections to $F_2^D(x)$. The total contribution to the deuteron structure function from meson exchange is:

$$\delta^{(M)} F_2^D(x, Q^2) = \sum_M \int_x^1 dy f_{M/D}(y) F_2^M(x/y, Q^2), \quad (20)$$

where $M = \pi, \rho, \omega, \sigma$. The virtual meson structure function, F_2^M , one approximates by the (real) pion structure function, data for which exist from Drell-Yan production. The exchange-meson distribution functions $f_M(y)$ are obtained from the non-relativistic reduction of the nucleon—meson interaction given in Refs. [30,36]. In practice pion exchange is the dominant process, and this gives a positive contribution to $\delta^{(M)} F_2^D(x, Q^2)$. The exchange of the fictitious σ meson (which represents correlated 2π exchange) also gives rise to antishadowing for small x . Vector mesons (ρ, ω) exchange cancels some of this antishadowing, however the magnitude of these contributions is smaller. In fact, for soft meson—nucleon vertices ($\Lambda_M \lesssim 1.3 \text{ GeV}$) all contributions other than that of the pion are totally negligible.

B. Neutron Structure Function at Small x

For $x \lesssim 0.1$ the magnitude of the (negative) Pomeron/VMD shadowing is larger than the (positive) meson-exchange contribution, so that the total $\delta^{(\text{shad})} F_2^D$ is negative. For larger x ($\approx 0.1 - 0.2$) there is a very small amount of antishadowing, which is due mainly to the VMD contribution, and also to the pion-exchange contribution. For the NMC kinematics

($x > 0.004$, $Q^2 = 4 \text{ GeV}^2$) [37], the overall effect on the shape of the neutron structure function is a 1 – 2% increase in $F_2^n/F_2^{n,\text{bound}}$ for $x \lesssim 0.01$, where $F_2^{n,\text{bound}} \equiv F_2^D - F_2^p$. The presence of shadowing in the deuteron would be confirmed through observation of a deviation from unity in the F_2^D/F_2^p structure function ratio in the kinematic region where Regge theory is expected to be valid. Although the exact value of x below which the proton and (free) neutron structure functions become equivalent is not known, it is expected that at low enough x , $F_2^p \rightarrow F_2^n$, in which case $F_2^D/F_2^p \rightarrow 1 + \delta^{(\text{shad})} F_2^D/F_2^p$. While for the lowest NMC data point it may be debatable whether the Regge region is reached, the E665 Collaboration [38] has taken data to very low x , $x \sim 10^{-5}$, which should be much nearer the onset of Regge behavior.

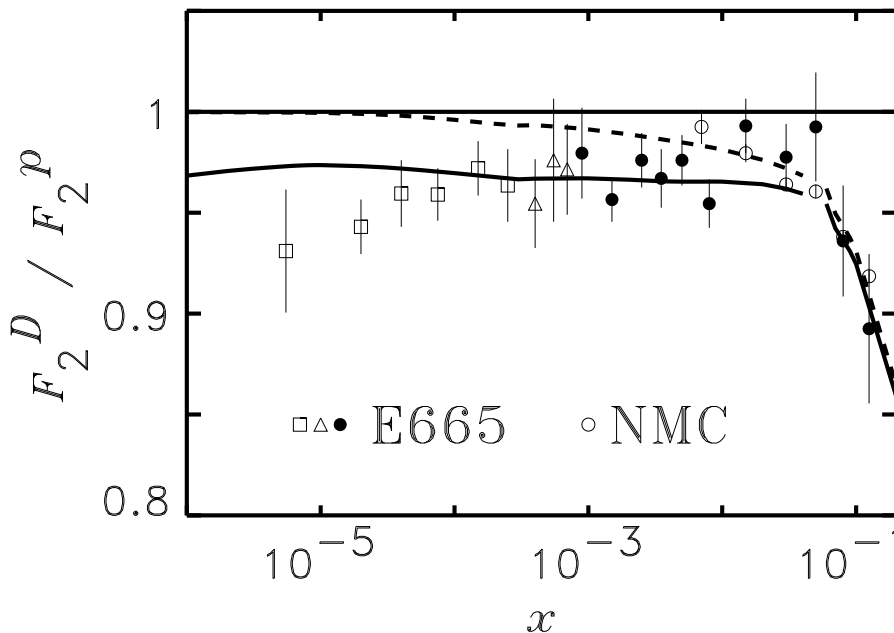


FIG. 5. x dependence of the D/p structure function ratio, compared with the low- x E665 data [38] and NMC data [37] at larger x . The dashed curve is the result without any shadowing correction.

In Fig.5 we show the low x E665 Collaboration data [38], as well as the earlier NMC data at larger x [37] (note that the E665 data are not taken at fixed Q^2). The calculated ratio with a small shadowing correction is shown by the solid curve, while the result for the case of no shadowing is indicated by the dashed curve. Assuming $F_2^p = F_2^n$ in the lowest x -bins, the data clearly favor the shadowing scenario.

C. Are 1% Effects Worth Worrying About? – Gottfried Sum Rule

The main interest in the NMC measurement of the neutron structure function at low x was to test accurately the Gottfried sum rule,

$$S_G = \int_0^1 dx \frac{F_2^p(x) - F_2^n(x)}{x} \quad (21a)$$

$$= \frac{1}{3} - \int_0^1 dx (\bar{d}(x) - \bar{u}(x)) \quad (21b)$$

which, in the naive quark model where $\bar{d} = \bar{u}$, is $S_G^{\text{qm}} = 1/3$. Ignoring nuclear effects, the experimental value obtained by the NMC was $S_G^{\text{exp}} = 0.258 \pm 0.017$, indicating a violation of SU(2) flavor symmetry in the proton's sea. However, because the structure function difference in S_G is weighted by a factor $1/x$, any small differences between F_2^n and $F_2^{n,\text{bound}}$ could be amplified for $x \rightarrow 0$.

Including the above shadowing correction, the overall effect on the experimental value for S_G ,

$$S_G = S_G^{\text{exp}} + \int_0^1 dx \frac{\delta^{(\text{shad})} F_2^D(x)}{x}, \quad (22)$$

is a reduction of between -0.010 and -0.026 , or about 4 and 10% of the measured value without putting in the shadowing correction [30]. Therefore a value that reflects the ‘‘true’’ Gottfried sum should be around $S_G \approx 0.2$. This is some 30% reduction from the naive quark model prediction, S_G^{qm} . Hence the tiny shadowing effect in the deuteron results in a more significant violation of flavor SU(2) symmetry in the proton sea.

IV. SUMMARY

In summary, we have reanalyzed the latest proton and deuteron structure function data at small and large x , in order to obtain more reliable information on the structure of the neutron in the $x \rightarrow 0$ and $x \rightarrow 1$ limits.

At small x , we have estimated the nuclear shadowing arising from the double scattering of the virtual photon from both nucleons in the deuteron. To cover the entire range of Q^2 accessible to current experiments, the γ^*N interaction is described in terms of the VMD model, which models the correlated $q\bar{q}$ pair excitations of the virtual photon, together with Pomeron exchange for the uncorrelated $q\bar{q}$ pair interactions with the nucleon. Such a hybrid model is particularly necessary if one is to reproduce the observed Q^2 dependence of the EMC ratio at small x [39]. In addition, we have also included contributions from the exchange of mesons, which effectively cancels as much as half of the shadowing from the VMD/Pomeron-exchange mechanisms alone. The net effect is a $\lesssim 1\%$ reduction of F_2^D for $x \sim 0.004$, or equivalently a $\lesssim 2\%$ increase in the neutron structure function over the uncorrected F_2^n . This is consistent with the recent measurement by the Fermilab E665 Collaboration [38] of the ratio F_2^D/F_2^p down to $x \sim 10^{-5}$, which deviates from unity by about 4%, and suggests the presence of shadowing in the deuteron. Although the absolute values of the shadowing corrections to F_2^D are small, because they are concentrated at small x , the effect on the Gottfried sum S_G is a further reduction of up to $\sim 10\%$ over the value measured by NMC [37].

Including all of the currently known nuclear effects in the deuteron at large x , namely Fermi motion, binding, and nucleon off-mass-shell effects, we find that the total EMC effect is $\sim 2\%$ larger than in previous calculations based on on-mass-shell kinematics, from which

binding effects were omitted. The larger deviation from unity for $0.5 \lesssim x \lesssim 0.8$ in F_2^D/F_2^N translates into an increase in the ratio F_2^n/F_2^p . Our results indicate that as $x \rightarrow 1$ the limiting value of F_2^n/F_2^p is above the previously accepted result of $1/4$, and broadly consistent with the perturbative QCD expectation of $3/7$. This also implies that the d/u ratio approaches a *non-zero* value of $1/5$ as $x \rightarrow 1$.

Finally, for definitive tests of the nuclear effects in the deuteron one would like model-independent information on the neutron at both low and high x . In principle, this can be achieved with high-precision data from neutrino-proton experiments, from which individual flavor distributions can be determined, and the neutron structure function inferred from charge symmetry. Unfortunately, both the statistics on the neutrino data and the coverage in x will not allow this in the near future. It has therefore been suggested that one might perform a series of semi-inclusive experiments on deuteron targets, measuring in coincidence both the scattered lepton and recoiling proton or neutron. This would help constrain the deuteron wave function over a large range of kinematics, and hence enable the y -dependence of the nucleon momentum distribution functions to be mapped out directly. Such experiments are already planned for CEBAF and HERMES [40], and should provide critical information on the size and importance of relativistic and other short-distance nuclear phenomena in the deuteron.

ACKNOWLEDGMENTS

We would like to thank S.A.Kulagin, G.Piller, A.W.Schreiber and W.Weise for their contributions to the issues discussed here. W.M. thanks the organizers of the IInd. Cracow Epiphany Conference on Proton Structure for their hospitality, and the H. Niewodniczański Institute of Nuclear Physics for support during the stay in Cracow. This research was partially supported by the Australian Research Council and the U.S. Department of Energy grant # DE-FG02-93ER-40762.

REFERENCES

- [1] R.L.Jaffe, in *Relativistic Dynamics and Quark-Nuclear Physics*, eds. M.B.Johnson and A.Pickleseimer (Wiley, New York, 1985); S.V.Akulichev, S.A.Kulagin and G.M.Vagradov, Phys.Lett. B 158 (1985) 485; G.V.Dunne and A.W.Thomas, Nucl.Phys. A455 (1986) 701; H.Jung and G.A.Miller, Phys.Lett. B 200 (1988) 351; F.Gross and S.Liuti, Phys.Rev. C 45 (1992) 1374; S.A.Kulagin, G.Piller and W.Weise, Phys.Rev. C 50 (1994) 1154.
- [2] S.Kulagin, W.Melnitchouk, G.Piller and W.Weise, Phys.Rev. C 52 (1995) 932.
- [3] W.W.Buck and F.Gross, Phys.Rev. D 20 (1979) 2361; J.A.Tjon, Nucl.Phys. A 463 (1987) 157C; D.Plumper and M.F.Gari, Z.Phys. A 343 (1992) 343; F.Gross, J.W.Van Orden and K.Holinde, Phys.Rev. C 45 (1992) 2094.
- [4] W.Melnitchouk, A.W.Schreiber and A.W.Thomas, Phys.Lett. B 335 (1994) 11.
- [5] W.Melnitchouk, A.W.Schreiber and A.W.Thomas, Phys.Rev. D 49 (1994) 1183.
- [6] L.L.Frankfurt and M.I.Strikman, Phys.Lett. 76 B (1978) 333; Phys.Rep. 76 (1981) 215.
- [7] L.W.Whitlow *et al.*, Phys.Lett. B 282 (1992) 475.
- [8] EM Collaboration, J.J.Aubert *et al.*, Nucl.Phys. B293 (1987) 740.
- [9] T.Uchiyama and K.Saito, Phys.Rev. C 38 (1988) 2245.
- [10] L.P.Kaptari and A.Yu.Umnikov, Phys.Lett. B 259 (1991) 155.
- [11] M.A.Braun and M.V.Tokarev, Phys.Lett. B 320 (1994) 381.
- [12] A.Bodek *et al.*, Phys.Rev. D 20 (1979) 1471; A.Bodek and J.L.Ritchie, Phys.Rev. D 23 (1981) 1070.
- [13] A.Yu.Umnikov, F.C.Khanna and L.P.Kaptari, Z.Phys. A 348 (1994) 211.
- [14] A.Höcker and V.Kartvelishvili, Manchester preprint MC-TH-95/15, LAL-95/55 (1995); V.Blobel, DESY preprint DESY-84-118 (1984).
- [15] NM Collaboration, M.Arneodo *et al.*, Preprint CERN-PPE/95-138 (1995).
- [16] F.E.Close, *An Introduction to Quarks and Partons* (Academic Press, 1979).
- [17] F.E.Close, Phys.Lett. 43 B (1973) 422.
- [18] R.Carlitz, Phys.Lett. 58 B (1975) 345.
- [19] F.E.Close and A.W.Thomas, Phys.Lett. B 212 (1988) 227.
- [20] G.R.Farrar and D.R.Jackson, Phys.Rev.Lett. 35 (1975) 1416.
- [21] S.J.Brodsky, M.Burkardt and I.Schmidt, Nucl.Phys. B441 (1995) 197.
- [22] J.Gomez *et al.*, Phys.Rev. D 49 (1994) 4348.
- [23] H.Abramowicz *et al.*, Z.Phys. C 25 (1983) 29.
- [24] L.L.Frankfurt and M.I.Strikman, Phys.Rep. 160 (1988) 235.
- [25] W.Melnitchouk, G.Piller and A.W.Thomas, Phys.Lett. B 346 (1995) 165.
- [26] SM Collaboration, D.Adams *et al.*, Phys. Lett. B 357 (1995) 248; E143 Collaboration, K.Abe *et al.*, Phys.Rev.Lett. 75 (1995) 25.
- [27] J.Kwiecinski and B.Badelek, Phys.Lett. B 208 (1988) 508.
- [28] J.Kwiecinski, Z.Phys. C 45 (1990) 461.
- [29] B.Badelek and J.Kwiecinski, Nucl.Phys. B370 (1992) 278; Phys.Rev. D 50 (1994) 4.
- [30] W.Melnitchouk and A.W.Thomas, Phys.Rev. D 47 (1993) 3783.
- [31] W.Melnitchouk and A.W.Thomas, Phys.Lett. B 317 (1993) 437.
- [32] V.R.Zoller, Z.Phys. C 54 (1992) 425; G.Piller, W.Ratzka and W.Weise, Z.Phys. A (1995), in print; H.Khan and P.Hoodbhoy, Phys.Lett. B 298 (1993) 181.
- [33] H1 Collaboration, T.Ahmed *et al.*, Phys.Lett. B 348 (1995) 681.

- [34] A.Donnachie and P.V.Landshoff, Phys.Lett. B 191 (1987) 309.
- [35] A.Donnachie and P.V.Landshoff, Z.Phys. C 61 (1994) 139.
- [36] L.P.Kaptari, A.I.Titov, E.L.Bratkovskaya and A.Yu.Umnikov, Nucl.Phys. A 512 (1990) 684.
- [37] NM Collaboration, M.Arneodo *et al.*, Phys.Rev. D 50 (1994) 1.
- [38] E665 Collaboration, M.R.Adams *et al.*, Phys.Rev.Lett. 75 (1995) 1466; Phys.Lett. B 309 (1993) 477.
- [39] W.Melnitchouk and A.W.Thomas, Phys.Rev. C 52 (1995) 3373.
- [40] S.Kuhn *et al.*, CEBAF proposal PR-94-102.